

Precisely controlling the twist angle of epitaxial MoS_2/graphene heterostructure by AFM tip manipulation

Jiahao Yuan(袁嘉浩), Mengzhou Liao(廖梦舟), Zhiheng Huang(黄智恒), Jinpeng Tian(田金朋), Yanbang Chu(褚衍邦), Luojun Du(杜罗军), Wei Yang(杨威), Dongxia Shi(时东霞), Rong Yang(杨蓉), and Guangyu Zhang(张广宇)
Citation: Chin. Phys. B, 2022, 31 (**8**): 087302. DOI: 10.1088/1674-1056/ac720e
Journal homepage: http://cpb.iphy.ac.cn; http://iopscience.iop.org/cpb

What follows is a list of articles you may be interested in

Optical conductivity of twisted bilayer graphene near the magic angle

Lu Wen(文露), Zhiqiang Li(李志强), and Yan He(贺言)
Chin. Phys. B, 2021, 30 (**1**): 017303. DOI: 10.1088/1674-1056/abb65d

Twistronics in graphene-based van der Waals structures

Ya-Ning Ren(任雅宁), Yu Zhang(张钰), Yi-Wen Liu(刘亦文), and Lin He(何林)
Chin. Phys. B, 2020, 29 (**11**): 117303. DOI: 10.1088/1674-1056/abbbe2

Emerging properties of two-dimensional twisted bilayer materials

Yang Cheng(程阳), Chen Huang(黄琛), Hao Hong(洪浩), Zixun Zhao(赵子荀), Kaihui Liu(刘开辉)
Chin. Phys. B, 2019, 28 (**10**): 107304. DOI: 10.1088/1674-1056/ab3e46

Pressure-mediated contact quality improvement between monolayer MoS_2 and graphite

Mengzhou Liao(廖梦舟), Luojun Du(杜罗军), Tingting Zhang(张婷婷), Lin Gu(谷林), Yugui Yao(姚裕贵), Rong Yang(杨蓉), Dongxia Shi(时东霞), Guangyu Zhang(张广宇)
Chin. Phys. B, 2019, 28 (**1**): 017301. DOI: 10.1088/1674-1056/28/1/017301

A facile and efficient dry transfer technique for two-dimensional Van der Waals heterostructure

Li Xie(谢立), Luojun Du(杜罗军), Xiaobo Lu(卢晓波), Rong Yang(杨蓉), Dongxia Shi(时东霞), Guangyu Zhang(张广宇)
Chin. Phys. B, 2017, 26 (**8**): 087306. DOI: 10.1088/1674-1056/26/8/087306

RAPID COMMUNICATION

Precisely controlling the twist angle of epitaxial MoS_2/graphene heterostructure by AFM tip manipulation

Jiahao Yuan(袁嘉浩)[1,2,†], Mengzhou Liao(廖梦舟)[1,2,5,†], Zhiheng Huang(黄智恒)[1,2], Jinpeng Tian(田金朋)[1,2], Yanbang Chu(褚衍邦)[1,2], Luojun Du(杜罗军)[1], Wei Yang(杨威)[1,2], Dongxia Shi(时东霞)[1,2], Rong Yang(杨蓉)[1,3,‡], and Guangyu Zhang(张广宇)[1,2,4,§]

[1] *Beijing National Laboratory for Condensed Matter Physics and Institute of Physics, Chinese Academy of Sciences, Beijing* 100190, *China*
[2] *School of Physical Sciences, University of Chinese Academy of Sciences, Beijing* 100049, *China*
[3] *College of Semiconductors (College of Integrated Circuits), Hunan University, Changsha* 410082, *China*
[4] *Songshan Lake Materials Laboratory, Dongguan* 523808, *China*
[5] *Department of Control Engineering, Faculty of Electrical Engineering, Czech Technical University in Prague, Czech Republic*

(Received 6 April 2022; revised manuscript received 11 May 2022; accepted manuscript online 23 May 2022)

Two-dimensional (2D) moiré materials have attracted a lot of attention and opened a new research frontier of twistronics due to their novel physical properties. Although great progress has been achieved, the inability to precisely and reproducibly manipulate the twist angle hinders the further development of twistronics. Here, we demonstrated an atomic force microscope (AFM) tip manipulation method to control the interlayer twist angle of epitaxial MoS_2/graphene heterostructure with an ultra-high accuracy better than 0.1°. Furthermore, conductive AFM and spectroscopic characterizations were conducted to show the effects of the twist angle on moiré pattern wavelength, phonons and excitons. Our work provides a technique to precisely control the twist angle of 2D moiré materials, enabling the possibility to establish the phase diagrams of moiré physics with twist angle.

Keywords: AFM tip manipulation, MoS_2/graphene heterostructure, twist angle, moiré superlattice

PACS: 73.43.Fj, 73.21.Cd, 73.20.At, 68.65.–k **DOI:** 10.1088/1674-1056/ac720e

1. Introduction

Because of the weak van der Waals (vdW) interactions, two-dimensional (2D) materials can be stacked together without the constraints of lattice matching[1] and thus possess a fascinating degree of freedom — interlayer twist angle.[2–5] Realizing precise control of the interlayer twist angle is of the utmost importance to engineer the twistronics and a variety of novel physical properties, such as unconventional superconductivity,[6] moiré excitons,[7] nonlinear optics[8] and magnetism.[9] For the most commonly used 'tear and stack' techniques,[6] although the interlayer twist angle can be controlled precisely in principle, the inevitable inhomogeneity of twist angle, interface bubble and the inability to manipulate it lead to poor reproducibility and hinder the further development of twistronics.[10–12] On the other hand, for the epitaxial growth method, 2D moiré superlattices with perfect interfaces can be obtained, but their interlayer twist angle is usually in the most stable thermodynamic configuration.[13,14] Remarkably, the recent advance shows that benefiting from the ultra-low interfacial friction,[15,16] the twist angle of 2D moiré materials can be manipulated by an atomic force microscope (AFM) tip,[17–21] endowing the possibility to continuously tune the twist angle with high accuracy.

In this work, we demonstrated the control of the twist angle of epitaxial MoS_2/graphene heterostructure with an ultra-high accuracy via AFM tip manipulation. High-quality MoS_2/graphene 2D heterostructures were epitaxially synthesized by chemical vapor deposition (CVD) to achieve clean and flat interfaces without bubbles. An AFM tip was used to control the interlayer twist angle. By precise manipulation of the AFM tip at the nanometer scale, we achieved accurate control of the interface twist angle with precision below 0.1°. Conductive AFM (C-AFM), Raman and photoluminescence (PL) spectroscopy were performed to show the effect of the twist angle on moiré pattern wavelength, phonons and excitons. The implementation of this technique will be very useful for the fabrication and study of 2D moiré material systems.

2. Experimental details

2.1. Epitaxial growth of samples

The MoS_2/graphene 2D heterostructure was grown by a home-made three-temperature-zone CVD system.[14] S (Alfa Aesar, 99.5%, 6–10 g) and MoO_3 (Alfa Aesar, 99.9995%, 20 mg) as precursors were placed in zone-I and zone-II. Graphite was mechanically exfoliated on a 300 nm SiO_2/Si substrate in zone-III. During growth, Ar/O_2 (gas flow rate,

[†] These authors contributed equally to this work.
[‡] Corresponding author. E-mail: ryang@iphy.ac.cn
[§] Corresponding author. E-mail: gyzhang@iphy.ac.cn

© 2022 Chinese Physical Society and IOP Publishing Ltd

325/1 sccm) was used as the carrier gas and the pressure was maintained at 1.00 Torr. The temperatures in the three zones were 120 °C, 565 °C and 960 °C, respectively, and the growth time was about 25 min.

2.2. Spectroscopic characterizations

A Horiba Jobin Yvon LabRAM HR-Evolution Raman system was used to carry out Raman and PL characterizations. The wavelength of the excitation laser was 532 nm.

2.3. AFM/C-AFM imaging and friction measurements

An Asylum Research Cypher S system was used to perform AFM imaging and friction measurements. AFM imaging and friction measurements used an AC200-TS-R3 tip of which the vertical and lateral sensitivity was 630.70 nN/V and 6632.43 nN/V.[15,22] C-AFM imaging used an ASYELEC-01-R2 tip with Ti/Ir coating and the 901.730 holder. All the measurements were performed in ambient conditions (20–25 °C and 10%–20% R.H.).

3. Results and discussion

As shown in Fig. 1(a), the epitaxial MoS_2 domains are about micron size and have both 0° and 60° orientations. AFM image of Fig. 1(b) shows that the thickness of MoS_2 domains is around 0.7 nm, indicating the monolayer nature. The interface of the sample is flat and clean. The Raman spectrum of Fig. 1(c) shows an E_{2g} peak at 383.0 cm^{-1} and an A_{1g} peak at 407.8 cm^{-1}. The PL spectrum has a strong A exciton peak at 661.4 nm. We can also see the G peak of graphene at 580.8 nm and the 2D peak at 621.8 nm, and the G/2D peak height ratio indicates that the graphene was only few-layered.[23,24] Since MoS_2 and graphene have a large lattice mismatch of 28.4%, the interface forms an incommensurate configuration, achieving structural superlubricity with ultra-low friction.[15,16,25] The friction properties of the heterogeneous interface were characterized by the lateral force mode of AFM. By pushing the boundary of the MoS_2 flake or dragging the sample to move back and forth with an AFM tip, the magnitude of the friction force at the sample interface can be measured by observing the abrupt change of the lateral force signal.[15] Figure 1(d) shows the variation of the friction force at the interface between a MoS_2 flake and graphene under different normal forces applied by the tip. It can be seen that the friction force at the interface does not vary significantly with the change of the tip load, and the average friction force is 10.56 nN, which is maintained at an extremely low level. The coefficient of friction (COF) at the interface is also only 1.48×10^{-4}, much less than 10^{-3}, which confirms the structural superlubricity property of the heterogeneous interface of MoS_2/graphene.

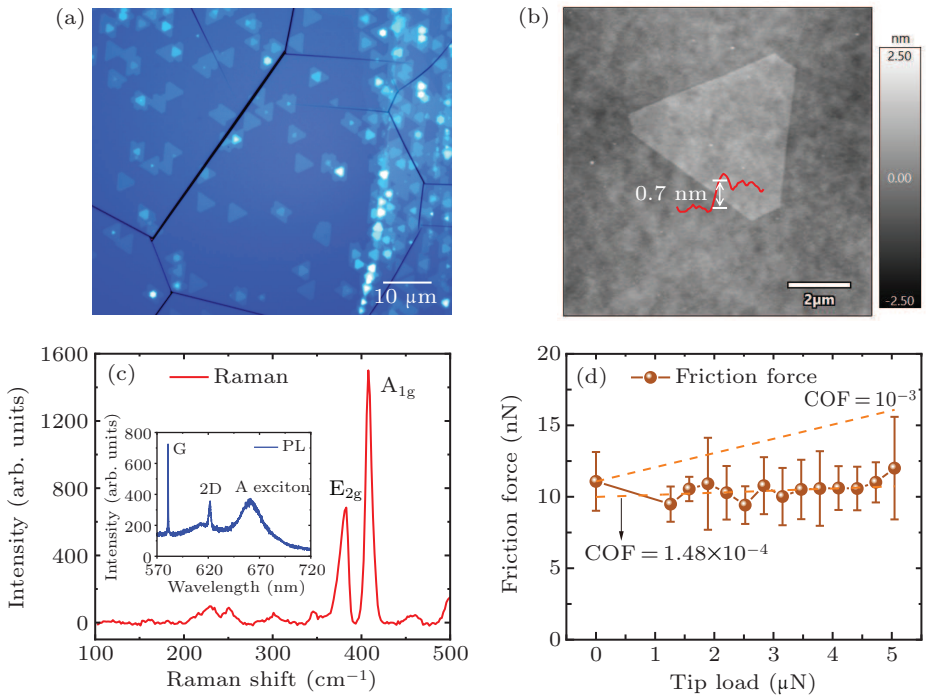


Fig. 1. Characterizations of MoS_2/graphene heterostructures. (a) Optical image of as-grown MoS_2 domains on few-layer graphene. (b) AFM image of a MoS_2 flake on a graphene substrate. (c) Raman and PL spectra of MoS_2/graphene heterostructures. (d) Friction force between MoS_2 and graphene as a function of tip load.

The superlubricity of MoS_2/graphene interface allows us to manipulate the twist angle with an AFM tip. First, the tapping mode of AFM should be used to obtain the topography of the sample. Then the AFM tip must be engaged in contact mode so that the tip can be in contact with the upper surface of graphene. We can manipulate the AFM tip to follow any path that we specify on the sample surface from one point to another point, either straight or curved. When the tip touches

the edge of the MoS_2 flake, due to the ultra-low friction at the MoS_2/graphene interface, the force exerted by the tip can drive the MoS_2 to move on the surface. However, as this system reaches the lowest energy state at 0°/60°,[14] a simple push by an AFM tip can only achieve a translational motion of the MoS_2 domains on graphene, rather than a rotation. Therefore, we need to add an extra external force to form a combined torque to control the twist angle of the heterogeneous structure. Figure 2(a) is a schematic illustration of the twist angle modulation method. In our experiments, we used the MoS_2 steps pinned at graphene boundaries and graphene wrinkles as the fulcrum for the rotation of MoS_2 and applied a pushing force with an AFM tip on the outside to generate a combined torque. By controlling the direction and route of the tip's movement, different twist angles can be achieved. Moreover, the accuracy of the angle control enabled by this AFM tip manipulation method can be very high. As shown in Fig. 2(b), point O, where the MoS_2 flake contacts the boundary edge, was set as the rotation axis. We used the AFM tip to push point A, the farthest point away from point O in this domain, and made it rotate along the normal direction of OA at 15 nm (Figs. 2(c)–2(d)). Since the length of OA was 8.97 μm, this MoS_2 flake rotated clockwise by 0.096°. By high-resolution scanning and finely controlling the path of the AFM tip, the accuracy of the twist angle modulation can reach an order of magnitude of 0.1° and even lower. Figures 2(e)–2(h) are the AFM images of the system achieving different twist angles under the manipulation of the AFM tip. We chose 9.0°, 36.0° and 61.5° as our targets and the results were in agreement with what we expected. It can be seen that by this approach, it is possible to achieve rotational control of the 2D heterostructure at any certain angles we want. Apart from MoS_2/graphene, AFM tip manipulation can also be applied to other vdW heterostructures and homostructures, e.g., bilayer graphene, to realize the high-precision controlling of the twist angle if the interface is clean and incommensurate.

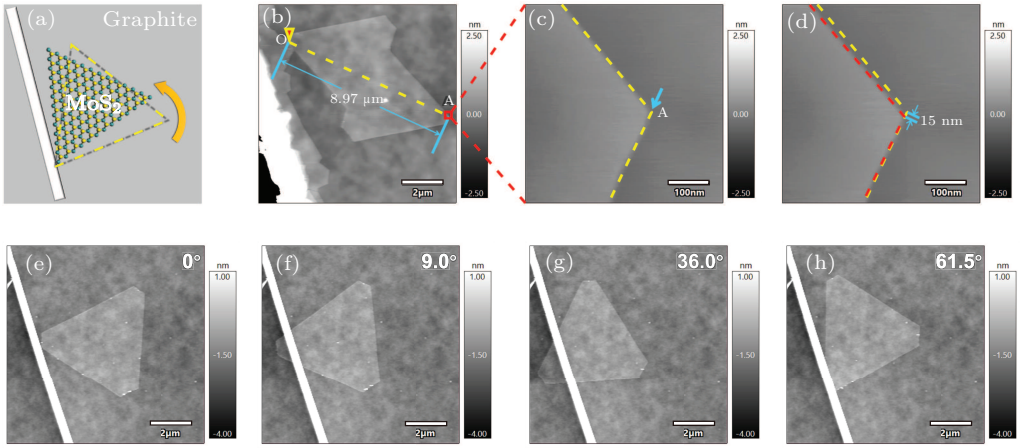


Fig. 2. Twist angle control of MoS_2/graphene heterostructure. (a) Schematic diagram of the method to control the twist angle between MoS_2 and graphene by an AFM tip. (b)–(d) A demonstration of precise control of interlayer twist angle below 0.1°. (e)–(h) AFM images of MoS_2/graphene heterostructure at different twist angles we want.

After achieving the precise control of the MoS_2/graphene twist angle by an AFM tip, we used C-AFM to characterize the heterostructure with different twist angles from 0° to 60°. The applied bias was 1.5 V with a current limit of ±20 nA and noise of 1.5 pA. A 110-MΩ resistor was connected in series into the circuit to prevent current overload. Figure 3(a) shows the C-AFM image of the 0° MoS_2/graphene sample. After a fast Fourier transform (FFT), two sets of hexagonal spots occurred (inset of Fig. 3(a)), corresponding to the moiré superlattice (red) and MoS_2 lattice (blue), respectively. Figures 3(b)–3(e) show the C-AFM images of MoS_2/graphene moiré patterns after the FFT filter at different twist angles, and it can be seen that the period of the moiré superlattice varies significantly at different angles, indicating the significant effect of the twist angle. The clear and regular moiré patterns confirm that the twist angle distribution in the heterostructure is uniform, and the interface is not contaminated. The moiré wavelength λ can be theoretically calculated by

$$\lambda = \frac{(1+\delta)a}{\sqrt{2(1+\delta)(1-\cos\theta)+\delta^2}},$$

where δ is the lattice mismatch between MoS_2 and graphene, a is the graphene lattice constant, and θ is the relative twist angle.[26] Figure 3(f) shows the theoretical and measured MoS_2/graphene moiré wavelength and MoS_2 lattice constants from 0° to 60°. For the moiré superlattice, the period first decreases and then increases gradually. It reaches the maximum at 0° and 60°, and the minimum around 30°, which is consistent well with the theoretical curves. Note that the lattice constant of MoS_2 does not change with the twist angle.

We also conducted spectroscopic characterizations of the MoS_2/graphene at different twist angles. Figures 4(a) and 4(b) show the Raman and PL spectra of the heterostructure modulated by the interlayer twist angle from 0° to 30°. The PL

spectra are normalized by the G peak of graphene. It can be seen that the peak shape of E_{2g} Raman mode, as well as the PL intensity and emission energy of the monolayer MoS_2, are strongly dependent on the twist angle. The peak of MoS_2 E_{2g} mode splits and broadens (inset of Fig. 4(c)) under in-plane strain resulted by moiré superlattice. As shown in Fig. 4(c), the splitting of E_{2g} peak decreases as the interlayer twist angle increases from 0° to 30°, revealing that the strain in MoS_2 is gradually getting smaller.[27,28] Also, as shown in Fig. 4(d), when the twist angle increases from 0° to 30°, the A exciton PL peak position is gradually blue-shifted, and its energy increases by 11.6 meV, which is either attributed to misorientation-induced lattice strain.[29] PL intensity of A exciton increases by a factor of 4.64 from 0° to 30° due to the transition of the MoS_2 band gap from indirect at 0° to direct at 30°.[30] These results are consistent with the previous work,[18] indicating that this twist angle control method can produce clean 2D moiré materials with highly precise and continuously controlled twist angle.

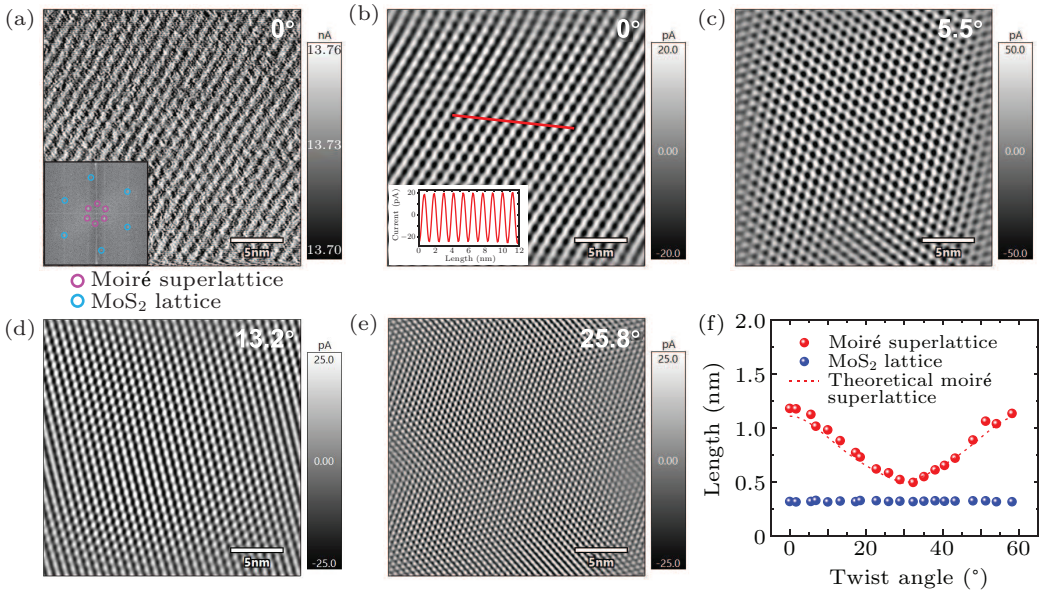


Fig. 3. C-AFM characterizations of MoS_2/graphene heterostructure. (a) C-AFM image of MoS_2/graphene at 0°. Inset is the pattern generated by FFT. (b)–(e) C-AFM image of MoS_2/graphene at different twist angles after FFT filter for MoS_2/graphene lattice. The inset of (b) is the cross-section along the red line. (f) Statistics of MoS_2/graphene moiré pattern periods and MoS_2 lattice constants from 0° to 60°.

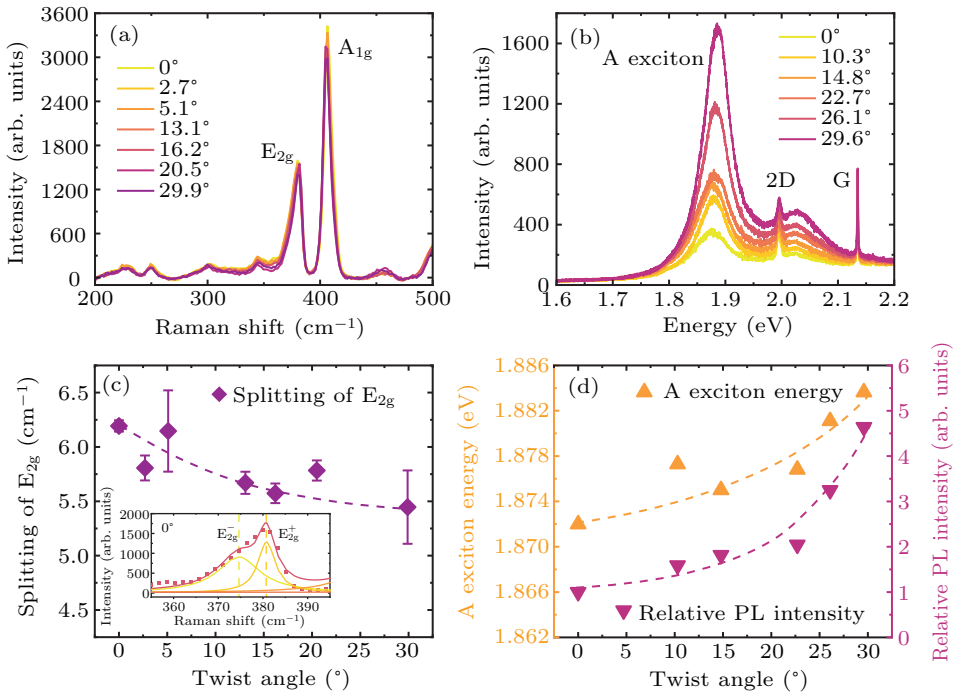


Fig. 4. Spectroscopic characterizations of the MoS_2/graphene heterostructure. Raman (a) and PL (b) of MoS_2/graphene at different twist angles. The splitting of E_{2g} mode peak (c), energy and relative PL intensity of A exciton (d) associated with the interlayer twist angle.

4. Conclusion and perspectives

In summary, we demonstrated a method to precisely control the interlayer twist angle of epitaxial MoS_2/graphene heterostructure by an AFM tip. This technique is convenient and suitable for other 2D moiré homo- and heterostructures with incommensurate interfaces. The accuracy of twist angle control enabled by this method can reach the order of 0.1° and even below. C-AFM, Raman and PL spectra were conducted to characterize the moiré patterns, phonons and excitons of MoS_2/graphene at different angles. Our work provides guidance for the fabrication of 2D twist-angle-dependent incommensurate homo- and heterostructures with clean interfaces and high angular accuracy and uniformity.

Acknowledgement

Project supported by the Natioanl Natural Science Foundation of China (Grant Nos. 62122084, 12074412, 61888102, and 11834017).

References

[1] Novoselov K S, Mishchenko A, Carvalho A and Castro Neto A H 2016 *Science* **353** 461
[2] He F, Zhou Y, Ye Z, Cho S H, Jeong J, Meng X and Wang Y 2021 *ACS Nano* **15** 5944
[3] Du L J, Hasan T, Castellanos-Gomez A, Liu G B, Yao Y G, Lau C N and Sun Z P 2021 *Nat. Rev. Phys.* **3** 193
[4] Andrei E Y and MacDonald A H 2020 *Nat. Mater.* **19** 1265
[5] Tang K W and Qi W H 2020 *Adv. Funct. Mater.* **30** 20
[6] Cao Y, Fatemi V, Fang S, Watanabe K, Taniguchi T, Kaxiras E and Jarillo-Herrero P 2018 *Nature* **556** 43
[7] Tran K, Moody G, Wu F, *et al.* 2019 *Nature* **567** 71
[8] Liu J P and Dai X 2020 *npj Comput. Mater.* **6** 10
[9] Lu X, Stepanov P, Yang W, Xie M, Aamir M A, Das I, Urgell C, Watanabe K, Taniguchi T, Zhang G, Bachtold A, MacDonald A H and Efetov D K 2019 *Nature* **574** 653
[10] Kazmierczak N P, Van Winkle M, Ophus C, Bustillo K C, Carr S, Brown H G, Ciston J, Taniguchi T, Watanabe K and Bediako D K 2021 *Nat. Mater.* **20** 956
[11] Purdie D G, Pugno N M, Taniguchi T, Watanabe K, Ferrari A C and Lombardo A 2018 *Nat. Commun.* **9** 5387
[12] Lau C N, Bockrath M W, Mak K F and Zhang F 2022 *Nature* **602** 41
[13] Yang W, Chen G, Shi Z, Liu C C, Zhang L, Xie G, Cheng M, Wang D, Yang R, Shi D, Watanabe K, Taniguchi T, Yao Y, Zhang Y and Zhang G 2013 *Nat. Mater.* **12** 792
[14] Yu H, Yang Z, Du L, Zhang J, Shi J, Chen W, Chen P, Liao M, Zhao J, Meng J, Wang G, Zhu J, Yang R, Shi D, Gu L and Zhang G 2017 *Small* **13** 1603005
[15] Liao M, Nicolini P, Du L, Yuan J, Wang S, Yu H, Tang J, Cheng P, Watanabe K, Taniguchi T, Gu L, Claerbout V E P, Silva A, Kramer D, Polcar T, Yang R, Shi D and Zhang G 2022 *Nat. Mater.* **21** 47
[16] Yuan J, Yang R and Zhang G 2021 *Nanotechnology* **33** 102002
[17] Wang D, Chen G, Li C, *et al.* 2016 *Phys. Rev. Lett.* **116** 126101
[18] Du L J, Yu H, Liao M Z, Wang S P, Xie L, Lu X B, Zhu J Q, Li N, Shen C, Chen P, Yang R, Shi D X and Zhang G Y 2017 *Appl. Phys. Lett.* **111** 263106
[19] Ribeiro-Palau R, Zhang C J, Watanabe K, Taniguchi T, Hone J and Dean C R 2018 *Science* **361** 690
[20] Finney N R, Yankowitz M, Muraleetharan L, Watanabe K, Taniguchi T, Dean C R and Hone J 2019 *Nat. Nanotechnol.* **14** 1029
[21] Hu C, Wu T, Huang X, Dong Y, Chen J, Zhang Z, Lyu B, Ma S, Watanabe K, Taniguchi T, Xie G, Li X, Liang Q and Shi Z 2022 *Sci. Rep.* **12** 204
[22] Higgins M J, Proksch R, Sader J E, Polcik M, Mc Endoo S, Cleveland J P and Jarvis S P 2006 *Review of Scientific Instruments* **77** 013701
[23] Ferrari A C, Meyer J C, Scardaci V, Casiraghi C, Lazzeri M, Mauri F, Piscanec S, Jiang D, Novoselov K S, Roth S and Geim A K 2006 *Phys. Rev. Lett.* **97** 187401
[24] Ferrari A C 2007 *Solid State Commun.* **143** 47
[25] Hod O, Meyer E, Zheng Q and Urbakh M 2018 *Nature* **563** 485
[26] Yankowitz M, Xue J M, Cormode D, Sanchez-Yamagishi J D, Watanabe K, Taniguchi T, Jarillo-Herrero P, Jacquod P and LeRoy B J 2012 *Nat. Phys.* **8** 382
[27] Conley H J, Wang B, Ziegler J I, Haglund R F, Jr., Pantelides S T and Bolotin K I 2013 *Nano Lett.* **13** 3626
[28] Zhu C R, Wang G, Liu B L, Marie X, Qiao X F, Zhang X, Wu X X, Fan H, Tan P H, Amand T and Urbaszek B 2013 *Phys. Rev. B* **88** 121301
[29] Liu G B, Xiao D, Yao Y, Xu X and Yao W 2015 *Chem. Soc. Rev.* **44** 2643
[30] Ebnonnasir A, Narayanan B, Kodambaka S and Ciobanu C V 2014 *Appl. Phys. Lett.* **105** 031603